

The κ -opioid receptor is primarily postsynaptic: Combined immunohistochemical localization of the receptor and endogenous opioids

(preprodynorphin/preproenkephalin/rat/guinea pig)

ULF ARVIDSSON*†, MAUREEN RIEDL*†, SUMITA CHAKRABARTI‡, LUCY VULCHANOVA*, JANG-HERN LEE*, ALBERT H. NAKANO*, XIAOQIN LIN*, HORACE H. LOH‡, PING-YEE LAW‡, MARTIN W. WESSENDORF*, AND ROBERT ELDE*§

Departments of *Cell Biology and Neuroanatomy and ‡Pharmacology, University of Minnesota, Minneapolis, MN 55455

Communicated by Tomas Hökfelt, Karolinska Institutet, Stockholm, Sweden, February 27, 1995

ABSTRACT Antisera were raised against a synthetic peptide corresponding to the carboxyl terminus of the κ -opioid receptor (KOR1). Specificity of the antisera was verified by staining of COS-7 cells transfected with KOR1 and epitope-tagged KOR1 cDNAs, by recognition by the antisera of proteins on Western blots of both transfected cells and brain tissue, by the absence of staining of both brain tissue and transfected cells after preabsorption of the antisera with the cognate peptide, and on the strong correlation between the distribution of KOR1 immunoreactivity and that of earlier ligand binding and *in situ* hybridization studies. Results indicate that KOR1 in neurons is targeted into both the axonal and somatodendritic compartments, but the majority of immunostaining was seen in the somatodendritic compartment. In sections from rat and guinea pig brain, prominent KOR1 staining was seen in the ventral forebrain, hypothalamus, thalamus, posterior pituitary, and midbrain. While the staining pattern was similar in both species, distinct differences were also observed. The distribution of preprodynorphin and KOR1 immunoreactivity was complementary in many brain regions, suggesting that KOR1 is poised to mediate the physiological actions of dynorphin. However, the distribution of KOR1 and enkephalin immunoreactivity was complementary in some regions as well. These results suggest that the KOR1 protein is primarily, but not exclusively, deployed to postsynaptic membranes where it mediates the effects of products of preprodynorphin and possibly preproenkephalin.

Three types of opioid receptors, μ , δ , and κ , mediate the diverse functional effects of opioids in both the peripheral and central nervous system. Physiological studies have found that the opioid receptors play important roles in modulation of neurotransmitter release, respiratory depression, modulation of pain perception, neuroendocrine secretion, and regulation of intestinal motility (1). To date, at least one gene encoding each type of opioid receptor has been cloned (2–5), and these receptors belong to the large family of G protein-coupled receptors with seven transmembrane domains.

Autoradiographic receptor binding studies show a widespread but discrete distribution of each of these three opioid receptors in the brain and spinal cord (6, 7). Also, mRNA encoding each of these opioid receptors has a correspondingly discrete localization (8–10). However, there is little information about the cellular targeting of the receptor proteins and their spatial relationship to endogenous ligands. To address these issues we have generated antisera against δ - and μ -opioid receptors for direct identification and localization of the receptor proteins in the brain and spinal cord (11–13). The

cloned δ -opioid receptor (DOR1) is targeted primarily into axons where it most likely functions presynaptically (11, 12), whereas the cloned μ -opioid receptor (MOR1) is preferentially targeted to the somatodendritic domain where it most likely functions postsynaptically (13). Thus, in spite of the high level of identity between DOR1 and MOR1 (56% at the amino acid level), they preferentially target into different neuronal processes. In the present study we have generated and characterized antisera to the rat κ -opioid receptor (KOR1; 59% identity to DOR1 and 55% identity to MOR1) in order to analyze the targeting and distribution of KOR1 in rat brain and spinal cord as well as its spatial relationship to opioid peptides. Since various guinea pig tissues have served as models for κ -opioid receptors (14), the distribution and targeting of KOR1 in guinea pig brain and spinal cord were also analyzed.

METHODS

Generation of Antisera. KOR1 antisera were produced as described for DOR1 and MOR1 (11–13) in New Zealand White rabbits against a 15-residue peptide corresponding to amino acids 366–380 (DPASMRDVGGMNKPV) of the cloned rat KOR1 (2, 15–18). Antisera against residues 235–248 (SQENPNTYSEDLDV) of rat preprodynorphin (ppDYN; ref. 19) were produced in guinea pigs (DH; Sasco, Omaha, NB). The use of antisera against cryptic regions of neuropeptide precursors has been described (20).

Cell Culture, Transfection, and Construction of Epitope-Tagged Opioid Receptors. COS-7 and Neuro2a cells were transfected with cDNAs encoding KOR1, MOR1, and DOR1 by electroporation or calcium phosphate precipitation (21). In addition cells were transfected with opioid receptor cDNA tagged with the human influenza virus hemagglutinin epitope (TAG; the tagged receptors are hereafter referred to as KORTAG, MORTAG, and DORTAG, respectively; see ref. 13).

Immunoblot Analysis. Immunoblotting was performed as described (22). Briefly, membrane fractions were prepared from wild-type Neuro2a cells, Neuro2a cells stably expressing KORTAG, and rat brain. The membrane fractions were separated on SDS/PAGE and transferred to membranes. Blots were blocked overnight with 10% dry milk in Tris-buffered saline and then incubated with KOR1 antisera at a dilution of 1:2000. Horseradish peroxidase-conjugated goat anti-rabbit IgG was used as secondary antibody at a 1:5000 dilution. Immunoreactive proteins were visualized with enhanced chemiluminescence (Amersham).

Abbreviations: KOR1, κ -opioid receptor; DOR1, δ -opioid receptor; MOR1, μ -opioid receptor; ppDYN, preprodynorphin; DYN, dynorphin; ir, immunoreactivity; TAG, human influenza virus hemagglutinin epitope.

†U.A. and M.R. contributed equally to this study.

§To whom reprint requests should be addressed.

The publication costs of this article were defrayed in part by page charge payment. This article must therefore be hereby marked "advertisement" in accordance with 18 U.S.C. §1734 solely to indicate this fact.

Immunocytochemistry. Transfected COS-7 cells, grown on coverslips, were fixed in 4% paraformaldehyde and 0.2% picric acid in 0.1 M phosphate buffer (pH 6.9) for 1 hr. The cells were incubated overnight at 4°C with primary antisera at the following dilutions: rabbit anti-KOR1 diluted 1:2000, rabbit anti-MOR1 diluted 1:5000 (13), rabbit anti-DOR1 diluted 1:1000 (11, 12). Monoclonal antibodies against TAG diluted to 2 µg/ml (clone 12CA5; Boehringer Mannheim) were used in double-labeling immunofluorescence experiments. Single-labeled cells were detected with cyanine 3.18-conjugated secondary antibodies (1:200; Jackson ImmunoResearch), whereas double-labeling was visualized with fluorescein isothiocyanate (1:100)- and lissamine rhodamine (1:100)-conjugated secondary antibodies.

Adult male rats (Sprague-Dawley; 150–200 g; $n = 8$) and guinea pigs (DH, 375–400 g; Sasco; $n = 4$) were anesthetized with chloral hydrate (350 mg/kg, i.p.) and perfused via the heart with fixative (same as above) and then with 10% (wt/vol) sucrose in PBS. Brain, spinal cord, and dorsal root ganglia were sectioned (14–50 µm) and incubated 24–48 hr at 4°C with rabbit anti-KOR1 diluted 1:2000, guinea pig anti-ppDYN diluted 1:500, rabbit anti-dynorphin (DYN) diluted 1:1000 (23), and/or mouse anti-enkephalin diluted 1:1000 (Sera-Lab, Crewley Down, Sussex, U.K.). Double- and triple-labeling experiments with these antisera were done as described (24). The double-labeled sections were visualized with fluorescein isothiocyanate (1:100)- and lissamine rhodamine (1:100)-conjugated secondary antibodies or cyanine 5.18 (1:200)- and cyanine 3.18 (1:200)-conjugated antibodies. Triple-labeling was visualized with cyanine 5.18-, cyanine 3.18-, and fluorescein isothiocyanate-conjugated antibodies. Control sections were incubated with antisera pretreated with homologous and heterologous peptides at concentrations of 1 nM to 1 mM.

Multicolor confocal laser microscopy (25) was done using the Bio-Rad MRC-1000 system equipped with a krypton/argon ion laser. Images were printed on a Fuji Pictography 3000 color printer.

In Situ Hybridization. *In situ* hybridization using rat brain sections was carried out as described (13, 26). An antisense RNA probe for rat KOR1 containing the complete coding region was used. After hybridization and washing, the sections were first apposed to Hyperfilm βmax film (Amersham) for 7

days and then dipped in NTB2 photographic emulsion (Kodak) and exposed for 21 days.

RESULTS

Characterization of Antisera. Antisera were raised in rabbits against the carboxyl terminus of KOR1, corresponding to residues 366–380. Cognate peptide concentrations of 1 to 100 nM blocked the staining in both brain sections and transfected cells. Shorter synthetic peptides (residues 366–373, 369–376, and 374–380) were unable to block the staining even at 1 mM. This suggests that the epitope for the KOR1 antisera encompasses most of the last 15 amino acids of the molecule.

The antisera stained only cells transfected with KOR1 (data not shown) or KORTAG (Fig. 1 *A* and *A'*) cDNA. Cells transfected with DORTAG and MORTAG cDNAs, although they were readily visualized with the antisera against TAG, were not stained with anti-KOR1 (Fig. 1 *B*, *B'*, *C*, and *C'*). Western immunoblotting of partially purified membrane proteins from Neuro2a cells stably transfected with KORTAG cDNA and probed with anti-KOR1 and anti-TAG demonstrated the presence of immunoreactive proteins with an estimated molecular mass of 52–57 kDa (Fig. 1*D*, lanes 2 and 4; arrow indicates probable polymer of these proteins at 110–140 kDa). No specific staining was seen in wild-type Neuro2a cells with either anti-KOR1 or anti-TAG antisera (Fig. 1*D*, lanes 1 and 3). Protein partially purified from rat brain and posterior pituitary showed KOR1 immunoreactivity (ir) in a zone from 55 to 65 kDa (Fig. 1*D*, lanes 5 and 6). The KOR1 cDNA clone predicts a protein with a molecular mass of ≈43 kDa; this mass difference is most likely the result of posttranslational modifications.

To analyze the spatial relationship of KOR1 to DYN, its putative endogenous ligand, antisera were generated in guinea pigs against the carboxyl-terminal portion of ppDYN (residues 235–248). The specificity of these antisera was tested by (i) absorption controls with the cognate peptide, (ii) comparison of the distribution of ppDYN ir in brain to the distribution of DYN ir using a well-characterized rabbit anti-DYN antisera (23), and (iii) simultaneous localization of the guinea pig anti-ppDYN and rabbit anti-DYN. The staining in brain tissue was blocked at peptide concentrations of 0.1 to 1 µM, and the distribution of ir using the guinea pig antisera was similar to the

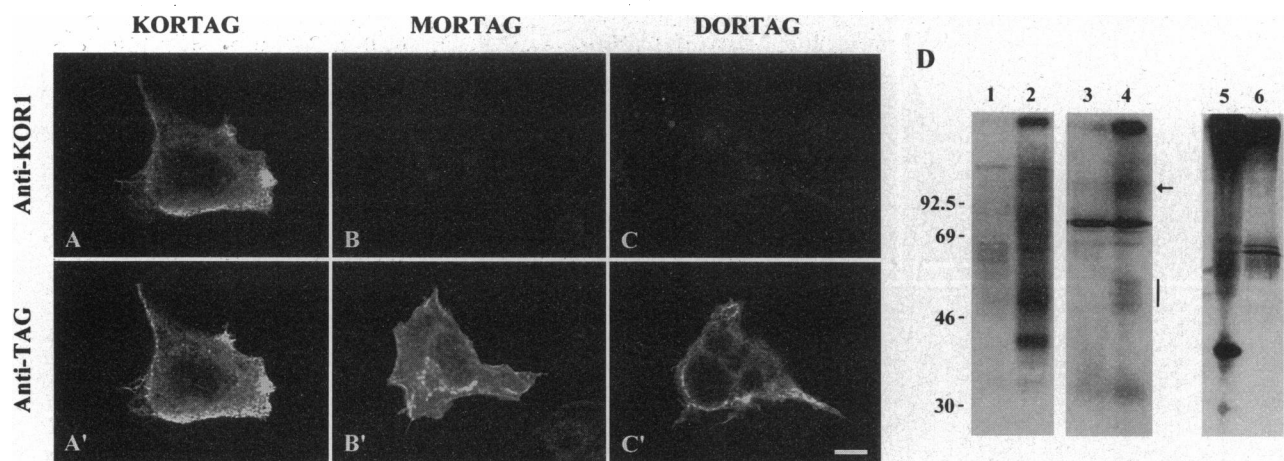


FIG. 1. Immunofluorescence confocal images of COS-7 cells transfected with KORTAG (*A* and *A'*), MORTAG (*B* and *B'*), and DORTAG (*C* and *C'*) cDNAs after incubation with a mixture of anti-KOR1 (*A*, *B*, and *C*) and anti-TAG (*A'*, *B'*, and *C'*). Anti-KOR1 stained only cells transfected with KORTAG cDNA (*A*) and coincided perfectly with the anti-TAG staining (*A'*). Intense TAG ir but no KOR1 ir was seen in the MORTAG cDNA (*B'*)- and DORTAG cDNA (*C'*)-transfected cells. (Bar = 10 µm.) (*D*) Western immunoblot of membrane proteins partially purified over a wheat germ lectin column from wild-type Neuro2a cells (lanes 1 and 3), stably transfected KORTAG Neuro2a cells (lanes 2 and 4), and rat brain and posterior pituitary (lanes 5 and 6) as probed with anti-KOR1 (lanes 1, 2, 5, and 6) and anti-TAG (lanes 3 and 4). No specific staining was seen in the wild-type Neuro2a cells (lanes 1 and 3); however, proteins around 52–57 kDa (indicated by a vertical bar) and a possible polymer at 110–140 kDa (indicated by an arrow) were recognized with both the anti-KOR1 (lane 2) and anti-TAG (lane 4) antisera. In membranes from rat brain and posterior pituitary, a zone around 55–65 kDa (indicated by a double vertical bar) was seen when probed with anti-KOR1 (lanes 5 and 6).

staining obtained using the rabbit antisera. This was also confirmed in the double-labeling experiments, although total coexistence was not seen.

Cellular Distribution and Targeting of KOR1 in Neurons. The KOR1 antisera stained a large number of cells and processes throughout the brain and spinal cord of rats and guinea pigs. Guinea pig tissue was preferred to that of rat for examination of the cellular distribution of KOR1 ir since the staining was more striking. An example of a KOR1-positive neuron from the guinea pig brain stem is shown in Fig. 2*A*. At higher magnification, the KOR1 labeling was seen in the plasmalemma of the soma (Fig. 2*B*) as well as in the membrane of the dendrites (Fig. 2*C*). In addition, KOR1 staining was seen as small puncta (200–400 nm) in the cytoplasm of the perikarya and within the dendrites (Fig. 2*B* and *C*). These puncta may represent vesicles transporting the receptor to or from its target. Some neurons exhibited KOR1 ir in dendritic spines (Fig. 2*D* and *E*). Instances of KOR1 ir in axonal processes were seen as well (Fig. 2*F*), but the majority of the neuronal processes stained with the KOR1 antisera appeared to be dendritic. A similar cellular distribution was also seen in rat tissue.

Localization of KOR1 in Brain and Spinal Cord. The distribution of KOR1 ir in the brain was strikingly similar to the distribution of κ -binding sites seen with ligand-binding autoradiography (6, 27). Dense KOR1 staining was seen in many regions including nucleus accumbens (Fig. 3*A*), olfactory tubercle including the islands of Calleja (Fig. 3*A*), ventral pallidum, caudate-putamen, bed nucleus stria terminalis, diagonal band, medial preoptic area, claustrum (Fig. 3*B*), endopiriform nucleus (Fig. 3*B*), insular cortex layers V and VI, subformal organ, paraventricular (Fig. 3*D*), periventricular, and supraoptic nucleus (Fig. 3*E*) as well as dorsomedial and arcuate nuclei of the hypothalamus, median eminence, posterior pituitary (Fig. 3*F*), amygdaloid nuclei (Fig. 3*G*), paraventricular nucleus of the thalamus, substantia nigra (Fig. 3*H*), interpeduncular nuclei, ventral tegmental area (Fig. 3*H*), regions of the trapezoid body (Fig. 3*J*), spinal trigeminal complex (Fig. 3*I*), nucleus of the solitary tract, spinal cord dorsal horn (Fig. 3*K*), area around the central canal (Fig. 3*L*), and dorsal root ganglion neurons (Fig. 3*M*). Many areas of the rat brain that contained mRNA encoding KOR1 also contained KOR1 ir, such as in claustrum (Fig. 3*B* and *C*).

The distribution of KOR1 ir in guinea pig coincides in almost all respects with the distribution of KOR1 mRNA reported in a previous study (28). However, KOR1 ir was not present in the claustrum and cerebellum despite mRNA coding for KOR1 in these areas. Comparison of the distribution of KOR1 ir in rat and guinea pig brain indicates that KOR1 ir is well conserved in these species with a few exceptions. For example, the claustrum, interpeduncular nuclei, dorsal horn of spinal cord, and area around the central canal were intensely stained with anti-KOR1 in rat (Fig. 3*K* and *L*) but not in guinea pig (Fig. 3*N* and *O*), whereas the suprachiasmatic nucleus and hippocampal formation did not show KOR1 ir in rat but were stained in guinea pig.

Spatial Distribution of KOR1 in Relation to Opioid Peptides. Double-labeled sections stained with both ppDYN and KOR1 antisera revealed regions of both high and low correlation in the brain and spinal cord. Both ppDYN and KOR1 ir were seen in nucleus accumbens (Fig. 4*A*), subformal organ, bed nucleus of stria terminalis, diagonal band, ventral pallidum, some amygdaloid nuclei, supraoptic nucleus, most areas of the hypothalamus, substantia nigra, spinal trigeminal complex, regions of the trapezoid body, nucleus of the solitary tract, and spinal cord dorsal horn (Fig. 4*B* and *C*). The islands of Calleja, claustrum, endopiriform nucleus, and interpeduncular nuclei contained high levels of KOR1 ir, but very little ppDYN ir, whereas the hippocampal formation and lateral hypothalamic nuclei contained ppDYN-ir but very little KOR1-ir. No unambiguous cases of coexistence were seen between ppDYN and KOR1, suggesting that KOR1 is not an autoreceptor for DYN. The spatial distribution of enkephalin in relation to KOR1 and ppDYN was also analyzed by simultaneous three-color immunofluorescence. The distribution of both ppDYN and enkephalin was complementary to that of KOR1 ir in some areas including the spinal cord dorsal horn (Fig. 4*D* and *D'*). In guinea pig brain, adjacent sections stained with DYN, KOR1, and enkephalin antisera revealed a spatial distribution similar to that seen in rat.

DISCUSSION

The specificity of the KOR1 antisera was evaluated using several criteria. First, the amino acid sequence to which the KOR1 antisera was raised is one of the few regions highly

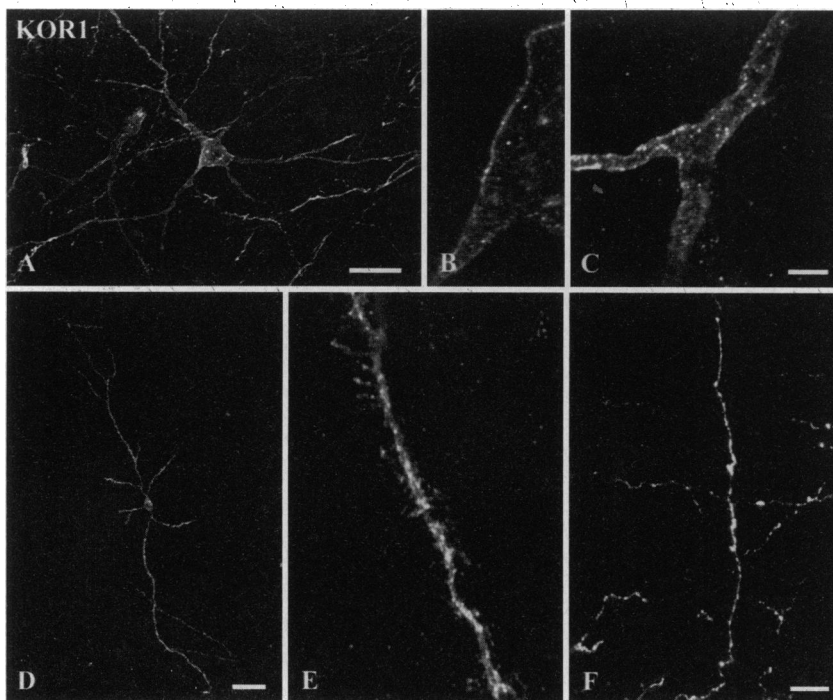


FIG. 2. Confocal micrographs showing the cellular localization of KOR1 ir in the brain of the guinea pig. KOR1-positive neurons (from brain stem in *A* and forebrain in *D*) express the receptor in the somatic plasmalemma (*B*), dendrites (*C*), dendritic spines (*D*) (magnified in *E*), and axons (*F*). Note KOR1-immunoreactive puncta (*B*, *C*, and *E*) possibly representing vesicles transporting the receptor to or from its target. (*A* and *D*, bars = 50 μ m; *B* = *C* = *E*, bar = 5 μ m; *F*, bar = 10 μ m.)

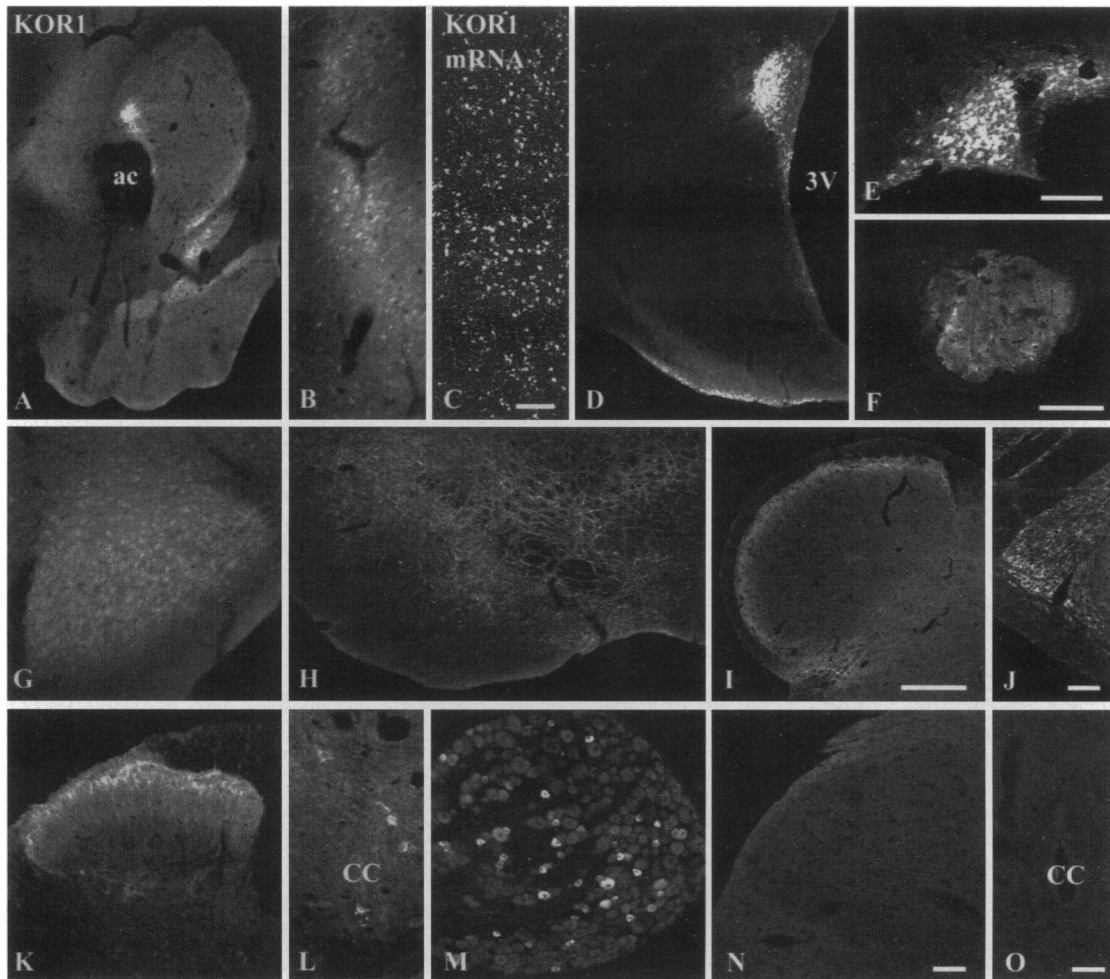


FIG. 3. Confocal micrographs showing the general distribution of KOR1 ir in the rat and guinea pig brain and spinal cord. KOR1 ir is shown in ventral forebrain (rat; *A*), claustrum (rat; *B*), hypothalamus (guinea pig; *D*), supraoptic nucleus (guinea pig; *E*), posterior pituitary (guinea pig; *F*), amygdaloid complex (rat; *G*), substantia nigra pars reticulata and ventral tegmental area (guinea pig; *H*), spinal trigeminal nucleus (rat; *I*), part of trapezoid body (rat; *J*), spinal cord dorsal horn (rat; *K* and guinea pig; *N*), area around the central canal (rat; *L* and guinea pig; *O*), and dorsal root ganglion (rat; *M*). The expression of mRNA encoding KOR1 in the claustrum is shown in *C*. ac, Anterior commissure; CC, central canal; 3V, third ventricle. (*A* = *D* = *H* = *I*, *F*, bars = 500 μ m; *E* and *J*, bars = 250 μ m; *B* = *C*, *G* = *K* = *M* = *N*, bars = 100 μ m; *L* = *O*, bar = 50 μ m.)

divergent among the opioid receptors, making it likely that anti-KOR1 would not recognize MOR1 or DOR1. Indeed, cells transfected with DOR1 or MOR1 were not stained by the

KOR1 antisera, but cells transfected with KOR1 stained intensely with anti-KOR1. Second, as determined by immunoblot analysis, the antisera recognized KOR1 in transfected

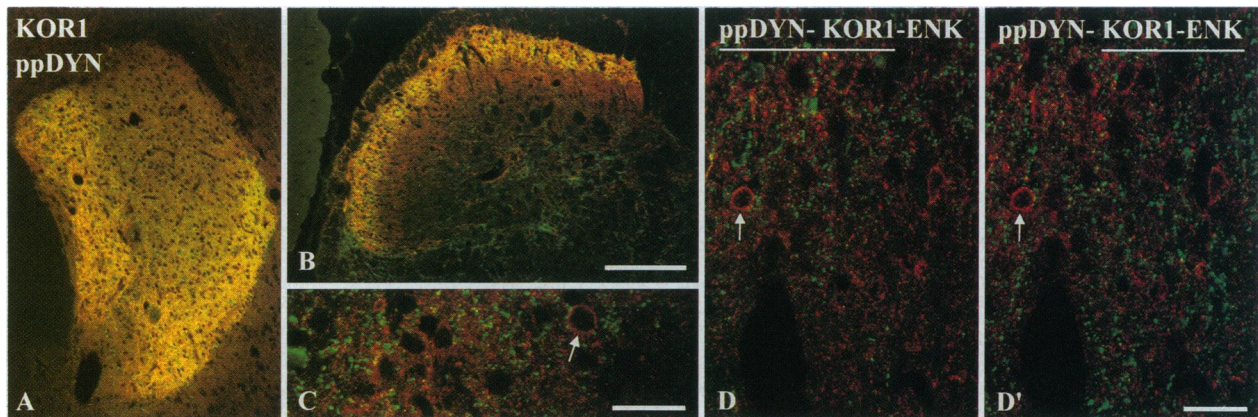


FIG. 4. Confocal micrographs showing the spatial distribution of KOR1 (red) ir in relation to opioid peptides (green) staining in the rat nucleus accumbens (*A*) and spinal cord dorsal horn (*B*–*E*). (*A*–*C*) Double-labeled sections stained for KOR1 and ppDYN. Yellow in *A* and *B* represents overlapping distribution at this low magnification and not coexistence. Note in *C* (higher magnification of the dorsal horn) close apposition of ppDYN-positive terminals to KOR1-stained cell membranes (arrow). (*D* and *D'*) Triple-labeled section stained for KOR1, ppDYN, and enkephalin (ENK). The relationship between KOR1 and ppDYN and between KOR1 and enkephalin are shown in *D* and *D'*, respectively. Note the proximity of both opioid peptides to KOR1 ir in the dorsal horn (arrows). (*A* = *B*, bar = 250 μ m; *C*, *D* = *D'*, bars = 25 μ m.)

cells and in brain extracts. Third, staining with anti-KOR1 was blocked by preabsorption of the antisera with the cognate peptide. Finally, the distribution of KOR1 ir in brain and spinal cord is in general agreement with the localization of binding sites and mRNA encoding KOR1. Thus, it is likely that our KOR1 antisera recognize a bona fide KOR1.

We have recently described the cellular localization of MOR1 and DOR1 in neurons in brain and spinal cord (11–13). Interestingly, DOR1 was found predominantly in axons; rarely was it found in the somatodendritic compartment. In contrast, MOR1 was found predominantly in the somatodendritic compartment and occasionally in axons. From these studies, we concluded that DOR1 is poised to function primarily as a presynaptic receptor, whereas MOR1 is poised to act predominantly as a postsynaptic receptor. Both DOR1 and MOR1 ir were seen over small puncta (200–400 nm) in axons, possibly representing vesicles transporting the receptor to or from its target (i.e., the site at which it interacts with its ligand). In the present study, KOR1 was found to be predominantly directed to the somatodendritic compartment (i.e., a postsynaptic receptor), although axons (i.e., a presynaptic receptor) containing KOR1 ir were seen as well. Physiological studies suggest both a postsynaptic (29, 30) as well as a presynaptic (31) role for κ receptors, and the present data are in keeping with those results. It is interesting that while KOR1, DOR1, and MOR1 have 55–60% identity at the amino acid level, they are targeted differently in neurons. The mechanism(s) that underlie the targeting of receptors within neurons are not known.

The immunohistochemical localization of KOR1 protein in the brain and spinal cord described in the present paper complements and extends previous studies on κ -opioid receptor distribution. The overall distribution of KOR1 ir in both rat and guinea pig corresponds remarkably well with the distribution of binding sites (6, 27) as well as with localization of mRNA encoding KOR1 (9, 28). However, some regions (e.g., medial habenula and ventromedial nucleus of the hypothalamus) that showed a relatively high degree of binding with (–)-[³H]bremazocine (6, 27) did not show a high level of KOR1 ir. Some degree of mismatch was also seen between the localization of mRNA encoding KOR1 and KOR1 ir, most notably in the claustrum and cerebellum of the guinea pig, where the mRNA was abundant (28) but KOR1 ir was not. These findings suggest that KOR1 is only one subtype of κ -opioid receptor and that other isoforms or subtypes exist. The existence of other isoforms or subtypes is further suggested by the absence of KOR1 staining in guinea pig dorsal horn, since evidence for κ -opioid receptors has been reported in this tissue (30, 32, 33). The lack of KOR1 ir in areas expressing mRNA coding for KOR1 could also be explained by deployment of KOR1 into axons, but this explanation is not valid for the cerebellum, since KOR1 staining was not seen in the molecular layer.

DYN has been proposed as the most likely endogenous ligand for κ -opioid receptors based on binding studies and bioassays (34). In the present study, KOR1 and ppDYN ir were found in many of the same regions of the brain and spinal cord. A mismatch was also observed: KOR1-positive areas lacking ppDYN innervation include the claustrum, endopiriform nucleus, and interpeduncular nuclei, whereas ppDYN-positive regions lacking KOR1 ir were seen in the hippocampal formation and lateral hypothalamic nuclei. It is possible that other endogenous ligands and opioid receptors are present in these areas. A problem with studying possible ligands for opioid receptors is the divergence (an opioid peptide can interact with several opioid receptors with varying affinity) and convergence (several opioid peptides have the ability to act at a specific opioid receptor) exhibited by several of the opioid peptides in their interaction with opioid receptors (34). Interestingly, nerve terminals that contain preproenkephalin-derived peptides were observed in the vicinity of KOR1-positive membranes. Some of the extended forms of enkepha-

lins have significant affinity for κ -opioid receptors (34). Thus, non-DYN opioid peptides may, by virtue of their proximity, serve as physiologically relevant ligands for κ -opioid receptors.

This work was supported by Public Health Service Grants DA 06299, DA 05466, DA 07339, DA 08131, and DA 00564; the Swedish Medical Research Council Project 12X-6815; and the Minnesota Medical Foundation.

- Pasternak, G. W. (1988) *The Opiate Receptors* (Humana, Clifton, NJ).
- Yasuda, K., Raynor, K., Kong, H., Breder, C. D., Takeda, J., Reisine, T. & Bell, G. I. (1993) *Proc. Natl. Acad. Sci. USA* **90**, 6736–6740.
- Evans, C. J., Keith, D. J., Jr., Morrison, H., Magendzo, K. & Edwards, R. H. (1992) *Science* **258**, 1952–1955.
- Kieffer, B. L., Befort, K., Gaveriaux-Ruff, C. & Hirth, C. G. (1992) *Proc. Natl. Acad. Sci. USA* **89**, 12048–12052.
- Chen, Y., Mestek, A., Liu, J., Hurley, J. A. & Yu, L. (1993) *Mol. Pharmacol.* **44**, 8–12.
- Mansour, A., Khachaturian, H., Lewis, M. E., Akil, H. & Watson, S. J. (1987) *J. Neurosci.* **7**, 2445–2464.
- Mansour, A. & Watson, S. J. (1993) in *Handbook of Experimental Pharmacology*, ed. Herz, A. (Springer, Berlin), Vol. 1, pp. 79–102.
- Mansour, A., Thompson, R. C., Akil, H. & Watson, S. J. (1993) *J. Chem. Neuroanat.* **6**, 351–362.
- Mansour, A., Fox, C. A., Meng, F., Akil, H. & Watson, S. J. (1994) *Mol. Cell. Neurosci.* **5**, 124–144.
- Thompson, R. C., Mansour, A., Akil, H. & Watson, S. J. (1993) *Neuron* **11**, 903–913.
- Dado, R. J., Law, P. Y., Loh, H. H. & Elde, R. (1993) *NeuroReport* **5**, 341–344.
- Arvidsson, U., Dado, R. J., Riedl, M., Lee, J.-H., Law, P. Y., Loh, H. H., Elde, R. & Wessendorf, M. W. (1995) *J. Neurosci.* **15**, 1215–1235.
- Arvidsson, U., Riedl, M., Chakrabarti, S., Lee, J.-H., Nakano, A. H., Dado, R. J., Loh, H. H., Law, P.-Y., Wessendorf, M. W. & Elde, R. (1995) *J. Neurosci.*, in press.
- Smith, J. A. M. & Leslie, F. M. (1993) in *Handbook of Experimental Pharmacology*, ed. Herz, A. (Springer, Berlin), Vol. 1, pp. 53–78.
- Minami, M., Toya, T., Katao, Y., Maekawa, K., Nakamura, S., Onogi, T., Kaneko, S. & Satoh, M. (1993) *FEBS Lett.* **329**, 291–295.
- Meng, F., Xie, G. X., Thompson, R. C., Mansour, A., Goldstein, A., Watson, S. J. & Akil, H. (1993) *Proc. Natl. Acad. Sci. USA* **90**, 9954–9958.
- Nishi, M., Takeshima, H., Fukuda, K., Kato, S. & Mori, K. (1993) *FEBS Lett.* **330**, 77–80.
- Li, S., Zhu, J., Chen, C., Chen, Y. W., Deriel, J. K., Ashby, B. & Liu-Chen, L. Y. (1993) *Biochem. J.* **295**, 629–633.
- Douglass, J., McMurray, C. T., Garrett, J. E., Adelman, J. P. & Calavetta, L. (1989) *Mol. Endocrinol.* **3**, 2070–2078.
- Carr, F. E., Reid, A. H. & Wessendorf, M. W. (1993) *Endocrinology* **133**, 809–814.
- Chen, C. A. & Okayama, H. (1988) *Biotechniques* **6**, 632–638.
- Roerig, S. C., Loh, H. H. & Law, P. Y. (1992) *Mol. Pharmacol.* **41**, 822–831.
- Weber, E., Evans, C. J. & Barchas, J. D. (1982) *Nature (London)* **299**, 77–79.
- Wessendorf, M. W., Apple, N. M., Molitor, T. W. & Elde, R. P. (1990) *J. Histochem. Cytochem.* **38**, 1859–1877.
- Brelje, T. C., Wessendorf, M. W. & Sorenson, R. L. (1993) in *Cell Biological Applications of Confocal Microscopy*, ed. Matsumoto, B. (Academic, San Diego), pp. 97–181.
- Simmons, D. M., Arriza, J. L. & Swanson, L. W. (1989) *J. Histochemol.* **12**, 169–181.
- Unterwald, E. M., Knapp, C. & Zukin, R. S. (1991) *Brain Res.* **562**, 57–65.
- Xie, G.-X., Meng, F., Mansour, A., Thompson, R. C., Hoversten, M. T., Goldstein, A., Watson, S. J. & Akil, H. (1994) *Proc. Natl. Acad. Sci. USA* **91**, 3779–3783.
- Besse, D., Lombard, M. C., Zajac, J. M., Roques, B. P. & Besson, J. M. (1990) *Brain Res.* **521**, 15–22.
- Grudt, T. J. & Williams, J. T. (1993) *Proc. Natl. Acad. Sci. USA* **90**, 11429–11432.
- Mulder, A. H. & Schoffelmeer, A. N. M. (1993) in *Handbook of Experimental Pharmacology*, ed. Herz, A. (Springer, Berlin), Vol. 1, pp. 125–144.
- Sharif, N. A., Hunter, J. C., Hill, R. G. & Hughes, J. (1988) *Neurosci. Lett.* **86**, 272–278.
- Tiberi, M. & Magnan, J. (1990) *Mol. Pharmacol.* **37**, 694–703.
- Corbett, A. D., Paterson, S. J. & Kosterlitz, H. W. (1993) in *Handbook of Experimental Pharmacology*, ed. Herz, A. (Springer, Berlin), Vol. 1, pp. 645–679.